15TH IEA HEAT PUMP CONFERENCE
MAY 26–29, 2026 | HOFBURG
VIENNA 2026
DECARBONISATION THROUGH INNOVATION

# Optimization of the process design parameters in cascaded heat pump systems for steam generation using natural refrigerants

Philip Hofmann[a*], Tim Peil[a], Jan Esch[a], Fabian Ahrendts[a], Julia Riese[b]

[a]Fraunhofer Research Institution for Energy Infrastructures and Geotechnologies IEG, Am Hochschulcampus 1, 44801, Bochum
[b]Fluid Process Engineering, Paderborn University, Warburger Str. 100, 33098 Paderborn

**Abstract**

The reliance on fossil fuels in industrial steam generation necessitates innovative decarbonization strategies. Highly efficient heat pump systems present a promising alternative, where the selection of the refrigerants and the process design are crucial factors for economic and environmental sustainability. This paper investigates the systematic optimization of the internal process parameters (superheating, intermediate pressure level, mass flows) of various alternative double stage heat pump circuits and the intermediate temperature level between the high-temperature heat pump and the vapor compression system for maximizing the system performance like the COP or the VHC with respect to the selected refrigerant and the process restrictions.
Based on the heat demand of industrial processes, such as drying and rectification, specific process conditions on the source and sink sides are defined. The analysis is conducted using steady-state thermodynamic simulation models, relying on accurate thermophysical property data and (semi-)physical models of relevant plant components like compressors, heat exchangers and flash tanks. A particular focus is placed on the adaptation of advanced circuit concepts using hydrocarbons as refrigerant. The resulting highly non-linear optimization problems are solved using the Nelder-Mead method (Downhill-Simplex). Objective of this study is to quantify the overall performance gains and sustainability advantages of electrified industrial steam generation through the utilization of natural refrigerants and adaptive system integration, thereby enabling an accelerated market uptake of these novel technologies. Compared to conventional heat pumps, significantly higher temperature lifts of up to 90 K and COP improvements of up to 50% at specific operating points can be achieved. When combined with mechanical vapor recompression systems (MVR) to achieve higher temperature lifts, these configurations enable a substantial reduction in both the size and number of stages of the MVR units, while maintaining the overall COP of the cascade.



*Keywords: system optimization; natural refrigerants, advanced heat pump circuits, steam generating heat pumps*

## 1. Introduction

In high-income economies, process heat, predominantly in the form of steam, remains a major driver of primary energy use and $CO_2$ emissions. Germany, Europe's largest economy, consumed 543 TWh of process heat in 2022, with the bulk still generated from fossil fuels such as natural gas and coal. A significant efficiency potential lies in the temperature range below 200 °C, where high-temperature heat pumps (HTHP) could substitute up to 200 TWh of demand. [1] Process heat requirements are particularly concentrated in the chemical, paper, and food industries. Key operations, including distillation, evaporation, cooking, sterilization, and drying, fall within the sub-200 °C range, underscoring the strategic relevance of HTHP integration. Achieving climate targets while maintaining industrial competitiveness requires a swift substitution of fossil-based heat sources with highly efficient electrified systems. [2] [3]

* Corresponding author. Tel.: 4923433858245
*E-mail address:* Philip.Hofmann@ieg.fraunhofer.de



*15th IEA Heat Pump Conference 2026 - HTH2.4 - https://doi.org/10.23697/2vcv-tj41*

This study investigates the thermodynamic optimization of alternative HTHPs employing alkanes as natural refrigerants. Anticipating regulatory trends, such as the phase-out of high-GWP fluids and potential EU restrictions on PFAS-containing refrigerants, synthetic working fluids (HFCs, HFOs) are excluded to ensure future-proof concepts. [4] The large temperature lifts required in industrial applications pose major challenges, particularly for conventional single-stage HTHPs coupled with mechanical vapor recompression (MVR). Additional constraints arise from the thermophysical properties of alkanes, including tilted vapor domes and low volumetric heating capacities. Based on a recent literature review, optimized multi-stage configurations are derived and subjected to nonlinear mathematical optimization. Comparative analysis with standard systems reveals substantial efficiency gains. Unlike prior studies, which focused on isolated HTHP-configurations or refrigerant comparisons, this work highlights untapped optimization potential in terms of coefficient of performance (COP), volumetric heating capacity (VHC), and ultimately levelized cost of heat (LCOH), especially when integrating advanced heat pump concepts and blower MVR systems in industrial waste heat recovery.

## 2. Methodology

Mateo-Royo et al. derived that an alternative cycle using two compressor and a flash tank (FT) as a separator at the intermediate temperature level is suitable to achieve high COPs using R-600 and R-600a as refrigerant (II in Figure 1). [4] Sadeghi et al. implemented a similar system which superheats the refrigerant at both compressor inlets via two separate internal heat exchangers (IHX) using R-600 and R-601 to achieve a sink temperature of 160 °C with a temperature lift of 90 K (IV). [5] Subcooling of the liquid refrigerant after leaving the FT is utilized in both cycles to allow the preheating of the vapor phase at the lowest temperature stage. [6] conducted measurements and simulation on a similar circuit, the main difference lies within in the circumstance that the liquid refrigerant is supercooled after the condenser outlet before entering the FT (I)/(III).

Slight modifications are made for the purpose of standardization. Unlike in literature, in variant (IV) D-stage D-IHX (V2), only the partial gaseous mass flow 3' from the FT is superheated in the IHX. This serves to increase the logarithmic mean temperature difference (LMTD) in the IHX and reduce the size of the system, also due to the inevitably smaller volume flows, which is illustrated in Figure 1:

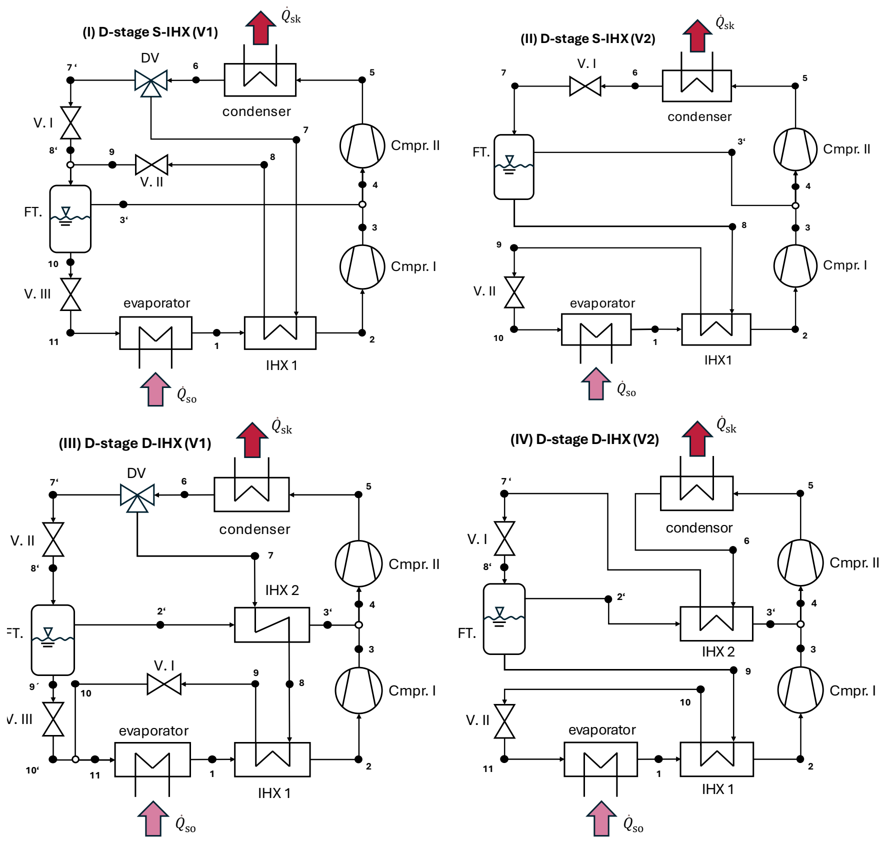


Figure 1: Visualization of the alternative HTHP-concepts designed for high temperature lifts using hydrocarbons

In variant V1, the mass flow is divided after the condenser. One part is subcooled in the IHX circuits, the other part is separated in the FT. In variant V2, the heat is always transferred to the next lower pressure level to minimize exergy losses. The subcooling of the liquid phase from the FT also reduces the enthalpy at the evaporator inlet, which can potentially increase the VHC and COP. Downstream of the condenser shown in Figure 1, an MVR system including a flash tank for steam generation and blowers could be installed.

### *2.1. Thermophysical properties of the selected refrigerants*

Hydrocarbons, particularly alkanes, are characterized by a wide temperature range suitable for heat pump applications. It can be observed that both the boiling point and the critical temperature increase with the number of carbon atoms. Due to weaker Van-der-Waals forces, iso-alkanes exhibit lower critical temperatures than n-alkanes with the same carbon atom number. [7] For steam generating HTHP-applications isobutane (R-600a), n-butane (R-600), isopentane (R-601a) and cyclopentane offer promising properties as shown in Table 1.

Table 1: Overview of the relevant properties of the selected natural refrigerants *[8]*, *[9]*

| substance | $T_{NBP}$ [°C] | $T_{crit}$ [°C] | $p_{crit}$ [bar] | GWP | $T_{AIT}$ [°C] | AHSRA class |
|---|---|---|---|---|---|---|
| isobutane (R-600a) | -11.75 | 134.67 | 36.29 | 3 | 460 | A3 |
| n-butane (R-600) | -0.49 | 151.98 | 37.96 | 4 | 368 | A3 |
| isopentane (R-601a) | 27.45 | 187.25 | 33.80 | 5 | 420 | A3 |
| cyclopentane | 48.85 | 238.57 | 45.71 | 11 | 320 | A3 |
| water (R-718) | 100 | 374.12 | 221.2 | ≈0 | - | A1 |

Assuming a Pinch-point temperature of 5 K in the heat exchanger (HEX) (e.g. evaporator and condenser) and a difference of 15 K between the critical temperature and the sink temperature and also the normal boiling point (NBP) as lower temperature limit , the selected refrigerants could theoretically cover a temperature range from -5 to 220 °C, even without an additional MVR system. This enables an adequate efficiency of a subcritical process on the one hand, whilst avoiding vacuum at low source temperatures on the other. [10] It has to be mentioned that all hydrocarbons are highly flammable, therefore ATEX precautions (Atmosphères Explosibles, Directive 2014/34/EU) must be conducted. [11]

### *2.2. Stationary modelling of HTHP- and MVR-system*

Stationary heat pump models are used in this paper since it can be assumed that many processes, especially in large companies, which stand for a major part of the process heat-consumption and chemical parks with their own steam supply networks, run continuously for the most part. All relevant components are implemented as semi-physical models. Compared to dynamic models, stationary models offer significantly shorter computing times and significantly reduce the complexity of following optimizations.

Pinch-point models are used for the condenser and evaporator and the internal heat exchangers (IHX). Each HEX is subdivided into up to three zones (gas, wet steam, and liquid), with a pinch-point temperature specified for each zone. Given the sink inlet temperature and the mass flow rates in both the refrigeration and sink circuits, the state variables of each circuit can be determined by solving the energy conservation equations. This method also allows pressure losses in the HEX to be considered. Constant losses of 5% are assumed, therefore the pressure ratio is globally set to $\boldsymbol{\Pi_{HEX} = 0.95}$.

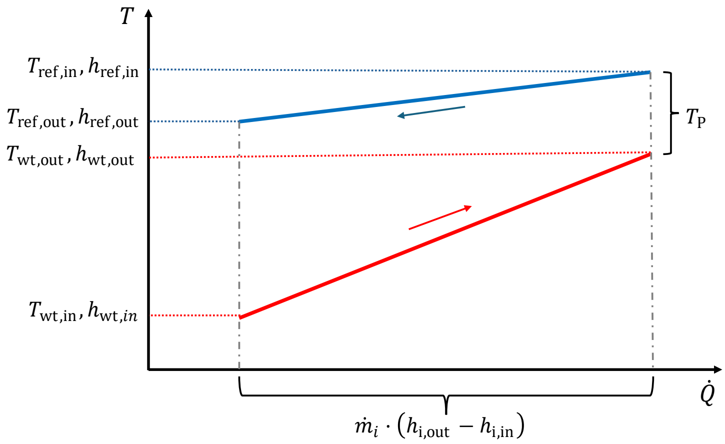

Figure 2: T,Q'-diagram of one zone of the condenser using a pinch-point approach. Red Line: pressurized water in the steam generating flash cycle, Blue Line: condensing refrigerant underlying pressure losses

The following equation derived from [12] describes the pinch-point model in one specific zone. In this context, the enthalpy flow of the water-driven source and sink circuits is equated to that of the refrigerant circuit, provided that the heat transfer condition, constrained by the pinch-point assumption, is satisfied.

$$\dot{m}_{\mathrm{wt}} \cdot \left(h_{\mathrm{wt,out}} - h_{\mathrm{wt,in}}\right) + \dot{m}_{\mathrm{ref}} \cdot \left(h_{\mathrm{ref,out}} - h_{\mathrm{ref,in}}\right) = 0$$
$$s.t.\ T_{\mathrm{ref,in}} - T_{\mathrm{wt,out}} \geq T_{\mathrm{P}},\ T_{\mathrm{ref,out}} - T_{\mathrm{wt,in}} \geq T_{P} \quad (1)$$

Modelling the efficiency of compressors is relevant for the accuracy of COP calculations. Many authors simplify matters by assuming constant efficiencies while others use pressure ratio-dependent approximations for a constant machine geometry. [4] This publication postulates that the machine geometry can be optimally designed for each operating point. However, higher pressure ratios can still be assumed to result in higher dissipation. Therefore, in accordance with [13], a reduction in isentropic efficiency of around 10 percentage points is assumed. The following assumptions are made:

$$\eta_{\mathrm{is,i}} = a + b \cdot \Pi_i + c \cdot \Pi_i^2$$
$$\eta_{\mathrm{is,i}} = 0.74 + 0.0121 \cdot \Pi_i - 3.72e-3 \cdot \Pi_i^2 \quad (2)$$

Losses in the powertrain of the compressor, like in the electric motor, the inverter and the bearings are assumed to be constant.

$$\eta_{\mathrm{m,i}} = 0.95$$
$$\eta_{\mathrm{Cmpr,i}} = \eta_{\mathrm{m,i}} \cdot \eta_{\mathrm{is,i}} \quad (3)$$

This approach allows the inclusion of the effects of different pressure ratios, arising from the choice of refrigerant and the placement of the intermediate pressure level, into the computed compressor efficiency.

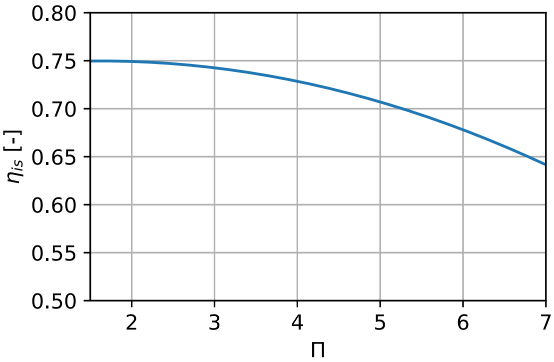

Figure 3: suggested isentropic efficiency $\eta_{is,i}$ for a (screw-) compressor

The FT, which is used in all alternative circuits and in the water circuit on the sink side for steam generation, is modelled as a separator. The following equations are assumed:

$$x_{\mathrm{FT}} = \frac{h_{\mathrm{FT}} - h'_{\mathrm{FT}}}{h''_{\mathrm{FT}} - h'_{\mathrm{FT}}}, \qquad x_{\mathrm{FT}} = \frac{\dot{m}''_{\mathrm{FT,out}}}{\dot{m}_{\mathrm{FT,in}}} \quad (4)$$

Pressure losses in the piping system are neglected. It is further assumed that the system operates continuously at its design point. Consequently, part-load effects in the compressor as well as in the heat exchangers (HEX, IHX) are disregarded.

### *2.3. Stationary modelling of a multi-stage MVR system*

A multi-stage blower MVR system is connected to the FT-cycle, which is used on the condenser side of the HTHP for steam generation. Since water (R718) overheats significantly during polytropic compression, liquid water is injected between the individual stages. This lowers the gas temperature to a defined superheating relative to the saturated vapor line and allows further cascaded recompression. Since the compression work for liquids is lower than for gases and no HEX is required, MVR systems deliver usually higher COPs than HTHP. However, the technical effort, the number of stages and the space requirements are higher than with HTHP, especially at lower source temperatures. This circumstance is attributed to the lower density of water vapor compared to other refrigerants.Equation 5 describes the required electrical power input per compressor stage (Cmpr). This formula is equally applicable for HTHP compressors.

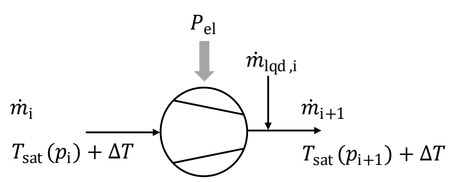

Figure 4: Scheme of an MVR stage.

$$h_{\text{Cmpr,re,i}} = \frac{h_{\text{Cmpr,is}}(p_{i+1}, s_i) - h_{\text{i}}}{\eta_{\text{is}}} + h_{\text{i}} = \frac{h_{\text{Cmpr,is}}(p_{i+1}, s_i) - h_{\text{i}}}{0.75} + h_{\text{i}}$$
$$P_{\text{Cmpr,i}} = \frac{1}{\eta_{m,i}} \cdot \dot{m}_i \cdot \left(h_{\text{Cmpr,re,i}} - h_{\text{i}}\right) \tag{5}$$

According to the specific enthalpy after compression $h_{\text{Cmpr,re,i}}$ the amount of cooling water is computed by using an energy conservation approach, which is commonly used for blower MVR: [14]

$$\dot{m}_{\text{lqd,i}} = \dot{m}_{\text{i}} \cdot \frac{h_{\text{i+1}}(T_{\text{sat}}(p_{\text{i+1}}) + \Delta T) - h_{\text{Cmpr,re}}}{h_{\text{lqd,i}} - h_{i+1}(T_{\text{sat}}(p_{\text{i+1}}) + \Delta T)} \tag{6}$$

In this study the isentropic efficiency for MVR-blowers is globally set to 75% and the maximum pressure ratio is set to 1.4, according to [11]. The number of stages required $n_{\text{stg}}$ and the pressure ratio per stage can be computed with equation 7 assuming a geometric pressure distribution. Ceiling the number of stages and using the geometric mean value results in a constant pressure ratio below the limitation for each stage.

$$\Pi = \frac{p_{\text{st,sk}}}{p_{\text{st,so}}} \Rightarrow n_{\text{stg}} = \text{ceil}\left[\log_{\Pi_{\max}}(\Pi)\right] \Rightarrow \Pi_{\text{stg}} = \Pi^{\frac{1}{n_{\text{stg}}}} \tag{7}$$

*2.4. Derivation and implementation of the optimization problem*

To achieve rapid decarbonization through HTHP systems, it is essential that the LCOH are competitive with fossil-based alternatives. The LCOH can be estimated in accordance with VDI Guideline 2067 and by applying suitable correlation curves. [15], [16] Two factors exert a particularly strong influence: consumption-related costs (OPEX), which are inversely proportional to the COP and investment costs (CAPEX), which scale with the size of key components such as compressors, piping, and heat exchangers. A meaningful reference parameter in this context is the VHC, which relates the volumetric flow rate at the compressor inlet to the thermal output delivered to the heat sink. [4], [17] The VHC [$\text{kJm}^{-3}$] is used instead of the heating capacity, as it is a specific parameter directly related to component sizing and its costs, while maintaining a constant heating capacity. During this optimization the capacity is set to be constant at 500 kW. While price-correlation approximations are often generic, the semi-physical models employed in this study allow an exact determination COP, and thus the Carnot efficiency as well as the VHC, under the assumptions made. Since the LCOH is highly nonlinear, non-convex, and discontinuous, the evaluation function applied in this study is based on Carnot efficiency, the VHC of both the HTHP and the MVR, as well as the number of stages in the MVR system. This approach establishes a direct link to the LCOH, while simultaneously reducing the complexity of the optimization.

The Carnot efficiency of the process remains more constant throughout a wide range of temperature lift by the heat pump and can be computed based on equation 8:

$$\eta_{C,\text{HTHP}} = \frac{COP}{COP_C} = \frac{\dot{Q}_{\text{sk}}}{\sum P_{\text{Cmpr}}} \cdot \frac{\left(T_{\text{sk,out}} - T_{\text{so,in}}\right)}{T_{\text{sk,out}}} \tag{8}$$

The VHC can be represented by the following equation. In multi-stage systems, the sum of all volumetric flow rates at the compressor inlets is considered.

$$VHC = \frac{\dot{Q}_{\text{sk}}}{\sum \dot{V}_{\text{Cmpr,in}}} \tag{9}$$

According to [18] the universal objective function adopted in this study is given by:

$$\begin{gathered}\min_{u \in U} \sum_{k=1}^{i} w_k \cdot n_k \cdot y_k = \vec{w} \odot \vec{n} \cdot \vec{y}(\vec{u},\vec{p}) \\ \mathrm{u} \in U \coloneqq \{u \in \mathbb{R}^k \mid u_i^{min} \leq u_i \leq u_i^{max}, i = \{1, \dots, k\}\}\end{gathered} \tag{10}$$

In this study, the universal approach is modified to impose stronger penalties on particularly low values of $\eta_{C,HTHP}$ and VHC. To this end, output variables targeted for maximization are treated as divisors, whereas those intended for minimization are defined as dividends. This leads to the following cost function:

$$\min_{u \in U} w_{\eta_C} \cdot \frac{n_{\eta_C}}{\eta_C(\vec{u},\vec{p})} + \sum w_{\mathrm{VHC,i}} \cdot \frac{n_{\mathrm{VHC,i}}}{VHC_{\mathrm{i}}(\vec{u},\vec{p})} + w_{\mathrm{stg,MVR}} \cdot n_{\mathrm{stg,MVR}} \tag{11}$$

As the alternative HTHP circuits are intended to be highly efficient the normalization is set to be $n_{\eta_C} = 0.5$. The VHC of hydrocarbons exhibits significant variation. While R-600a can achieve values exceeding 4000 kJ m⁻³ (based on a lift of 60 K and a sink temperature of 130 °C), the corresponding value for cyclopentane may fall below 1000 kJ m⁻³. To enforce a compact design, a reference value of 3000 kJ m⁻³ is adopted. As Blower MVRs deliver high volume flows, the reference for R-718 is set to 700 kJ m⁻³. This choice indirectly penalizes evaporating temperatures below the NBP, as such conditions inevitably result in unfavorable VHC values. [4]

### *2.5. Selection of an optimization algorithm and structure of the code*

Since the optimization problem is non-convex and the cost function is discontinuous and therefore not continuously differentiable, gradient-based optimizers are not applicable. [19] In this domain, genetic algorithms and nonlinear simplex methods such as Nelder–Mead are commonly recommended. [20] Due to its robustness and suitability for discontinuous objective functions, the Nelder-Mead algorithm implemented in the SciPy library is selected for this study. To further improve reliability and support convergence towards the global optimum, a preliminary grid search across the entire solution space is conducted.

As described in Figure 5 the code allows switching between the sole use of an HTHP or a cascade of HTHP and MVR, even during optimization. Upon completion of the grid search across all initial values, the global optimum is obtained by selecting the configuration associated with the lowest cost. Only the refrigerant must remain the same during optimization.

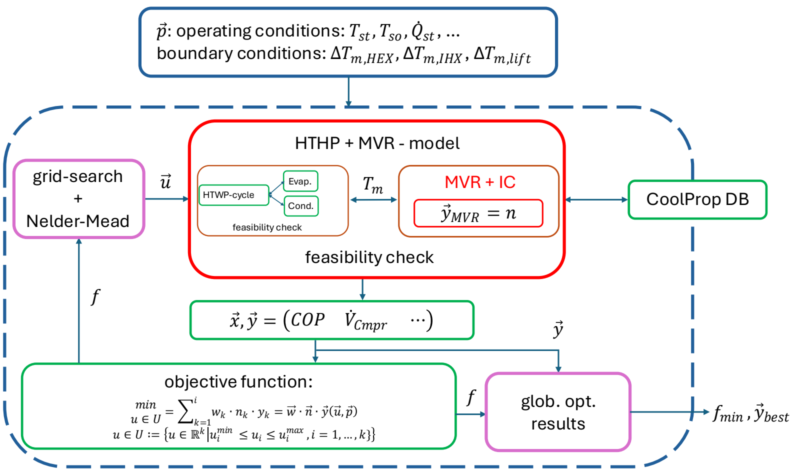

Figure 5: Flowchart of the optimization process using SciPy- and CoolProp-libaries *[9]*

If physically or technically infeasible states occur, such as compression into the wet-steam region, violation of energy conservation, or pinch-temperature constraints in the HEX/IHX, the value of the cost function is set to 1e6 as the Nelder-Mead algorithm does not respect constraints. The control vector $\vec{u}$ is defined individually depending on the HTHP layout: values are the superheating in the IHX, the mean pressure level in the HTHP-FT and the mass flow-ratio in the variants (I) V1 and (III) V1 as described in Figure 1. In the post-process the costs are compared between the refrigerants, to assume which one is the most promising.

## 3. Results and discussion

In the first part of this study, the potential of HTHP integration is assessed, while the evaluation of a downstream MVR system is deliberately omitted. A temperature lift limitation of 90 K is assumed. In the second part, the benefits of alternative HTHP configurations within an MVR cascade are compared to conventional arrangements. The operating points investigated appear promising for heat pump integration into rectification processes and centralized steam networks. For steam generation, a throttling of 5 K in the FT of the steam circuit is assumed. On the source side, a temperature difference of also 5 K is considered. This relatively small value is realistic for cooling systems in exothermic, temperature-sensitive processes and rectification columns. Since single-component refrigerants are considered, the pressure level in the evaporator and ultimately the COP is governed by the lowest temperature of the heat source. When transferring the results to processes with significant source temperature glide, the outflow temperature should be used as the reference parameter. Informed by practical experience the weight of Carnot-efficiency is set to 4, that of the VHC to 1, as efficiency usually has stronger influence on the LCOH, because consumption-related operating costs dominate in HTHP systems.

### *3.1. Direct HTHP-integration using alternative circuits*

The results for a weighting, which leads to reasonable refrigerant choices, are displayed in the figure below. The name of the optimal HTHP-circuit, the overall pressure ratio, the COP and the VHC are given. The COP and VHC are compared to a standard HTHP-cycle with an IHX employing the same refrigerant. It must be underlined that this is a theoretical study, as standard one-stage cycles might not reach such temperature lifts.

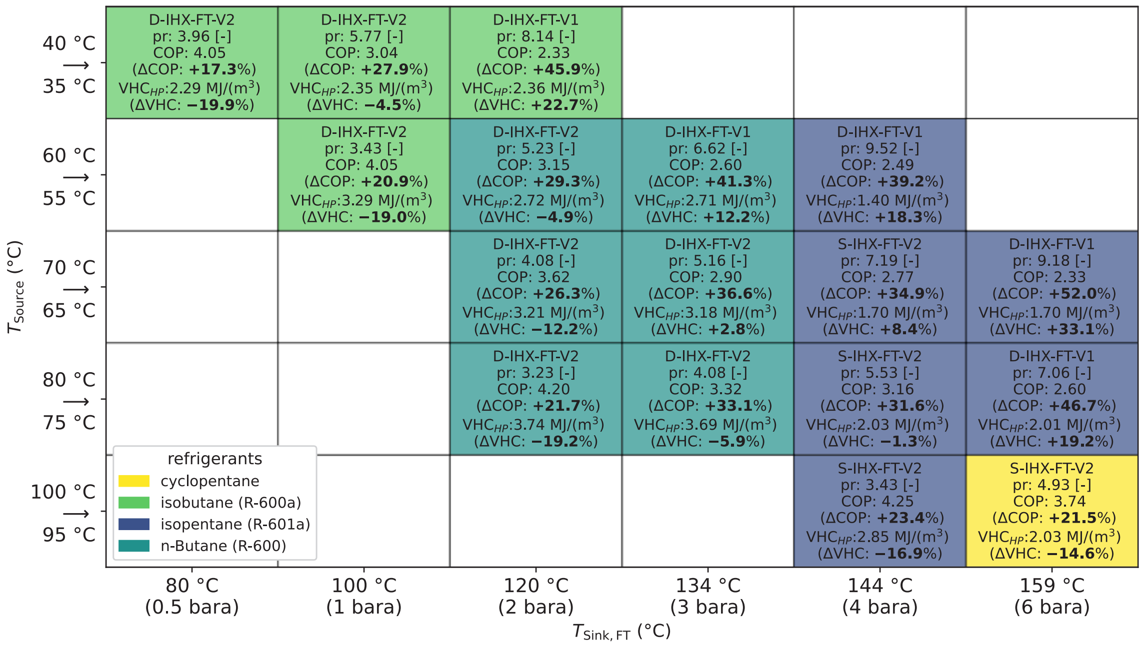


Figure 6: Optimal configurations for each operating point. The COP is improved up in a range from 17% to 52% and the ΔVHC varies in a range of -20% to 29%

The following assumptions are derivable from this HTHP-optimization:

- Although cyclopentane achieves the highest COPs for every operating point, it is reasonable to choose a refrigerant with a VHC of at least 1400 kJ/m$^3$.
- N-Butane is the refrigerant of choice to generate steam at 3 bar(a). Although the critical temperature is 152 °C, 4 bar(a) is not feasible due to the assumed losses in the condenser. Especially isopentane benefits from the alternative HTHP-cycles.
- The alternative circuits are less suitable for lifts lower than 60 K. Although the COP might increase by 20%, the VHC is lowered significantly in the same range. This is since the volume flow rate of the second compressor is also considered. The increased technical complexity can only be justified in scenarios with high sensitivity to operating cost.
- For higher lifts (>60 K) the alternative circuits outperform significantly regarding COP (>+30%) achieving also a lower VHC.

Furthermore, conclusions can be drawn regarding the suitability of specific configurations across different operating regimes. For temperature lifts exceeding 60 K, the (III) DS D-IHX FT-V1 configuration consistently outperforms, regardless of the selected refrigerant. In this regime, the optimizer exploits the upper boundary of 25 K superheating in the IHXs. As illustrated in Figure 7, this enables superheated refrigerant entering the condenser, particularly for R601a, where the isentropic curves intersect the tilted saturated vapor dome. Additionally, the vapor quality x at the evaporator inlet (pt. 11) is reduced, which positively affects both the VHC and the efficiency related COP.

At lower temperature lifts, the configurations (II) DS S-IHX FT-V2 and (IV) DS D-IHX FT-V2 prove advantageous. Across all simulated operating points, the optimizer applies only minimal additional superheating in IHX 2, thereby preventing compression into the saturated vapor region. In the case of DS S-IHX FT-V2, the intermediate pressure level is adjusted accordingly. Both cycles deliver nearly identical results, as IHX 2 is only used slightly. If high heat fluxes were transferred through IHX 2, the vapor quality in the FT inevitably decreases. As a result, a larger mass fraction of liquid refrigerant is expanded into the evaporator, leading to increased mass flow rates. This, in turn, raises the power consumption of the first compression stage and ultimately reduces both COP and VHC.

Table 2 gives an overview of the performance parameters of R601a in the different HTHP-cycles. In this case, as well as across all other scenarios, the (I) DS S-IHX FT-V1 configuration consistently exhibited inferior performance in terms of both COP and VHC. This can be attributed to a higher mass fraction flowing through the evaporator, which adversely affects system efficiency. It is also evident that for (IV) DS D-IHX FT-V2, the superheating in IHX 2 is negligible.

Table 2: performance data for each HTHP-cycle for Iso-Pentane (60 °C → 4 bar(a), ΔT: 84 K)

| HTHP cycle | COP [-] | $\eta_c$ [%] | VHC [kJ/m$^3$] | $\Delta T_{IHX1}$ [°C] | $\Delta T_{IHX2}$ [°C] | cost [-] |
|---|---|---|---|---|---|---|
| (I) DS S-IHX FT-V1 | 2.26 | 48.21 | 1258 | 25 | - | 6.76 |
| (II) DS S-IHX FT-V2 | 2.43 | 51.84 | 1403 | 25 | - | 6.22 |
| (III) DS D-IHX FT-V1 | 2.48 | 52.92 | 1402 | 25 | 25 | 6.13 |
| (IV) DS D-IHX FT-V2 | 2.43 | 51.84 | 1401 | 25 | 1 | 6.23 |

Figure 7 illustrates that the (III) DS D-IHX FT-V1 configuration enables enhanced internal thermal recuperation, resulting in a higher specific enthalpy at the condenser inflow (pt. 5) whilst achieving a nearly identical low specific enthalpy at the evaporator inflow (pt. 10 and 11 overlay each other).

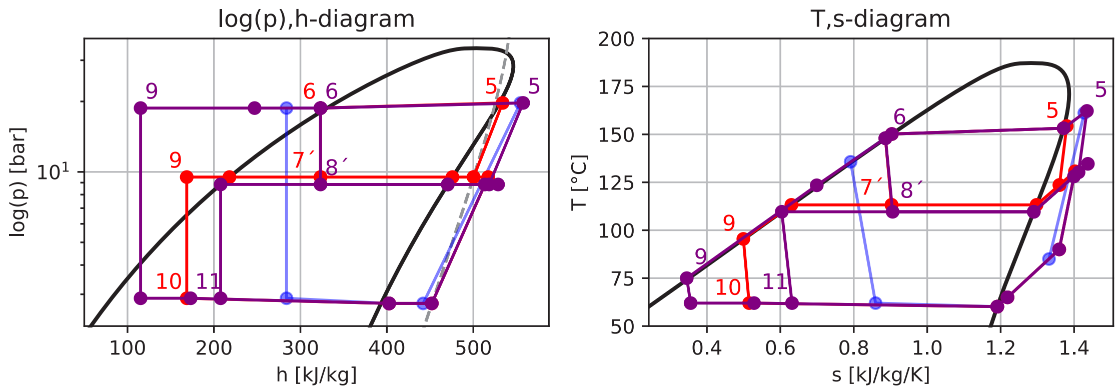


Figure 7: state charts of standard HTHP (blue), DS S-IHX FT V2 (red), DS D-IHX FT V1 (violet) for the process from Table 2 (**relevant state points**: 5: condenser in-, 6: condenser outflow; 7',8': flash tank; 9: IHX out; 10/11: evaporator in)

### *3.2. HTHP with cascaded blower MVR integration*

Rather than standalone integration, HTHPs are more commonly combined with downstream MVR-systems. This configuration enables overall extended temperature lifts exceeding 100 K. To identify optimal configurations, an operating point grid of source and sink temperatures is evaluated. The weight of Carnot-efficiency is set to 4.0, while the VHC of both the HTHP and MVR are weighed at 0.5, with each additional MVR stage penalized by 0.2. Conventional HTHPs are limited to a 50 K lift and a maximum of 15 K superheating in the IHX. Notably, regarding Figure , under these weighting conditions, only R-600a and R-600 are desired as working fluids, with R-600a dominating at source return temperatures below 40 °C.

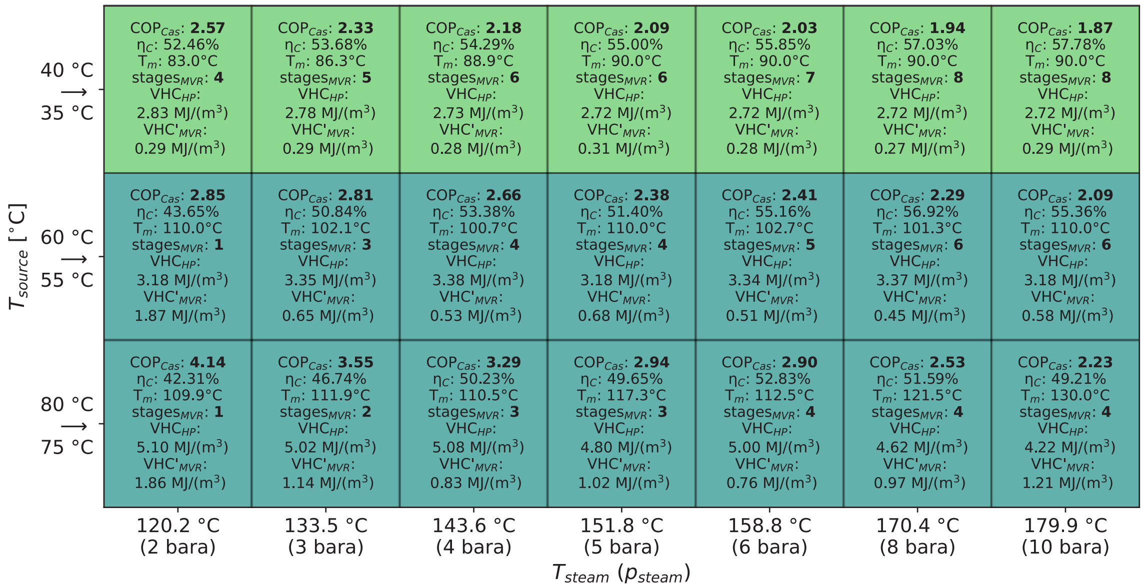


Figure 8: Optimized cascade of standard HTHP and blower MVR. The color-coding legend of the refrigerants refers to Figure 6

Applying these weights to the alternative cycles the number of MVR-blowers is reduced significantly; in a range from 1 to 5, with a median of 3. As the intermediate temperature for steam generation is higher, the VHC of the MVR-systems increases drastically, due to the higher density of water and the lower number of stages required. On the other hand, the HTHP-cycle becomes larger, as the VHC of the HTHP decreases, when a refrigerant with a higher critical temperature is chosen in most cases (despite $T_{source}$: 60 °C →55 °C) and a second compressor stage is added. The overall COP of the cascaded system does not change significantly when an alternative HTHP is used. It varies within a range of -3.1% to 14.7%, with a mean of 2.4%. For all cases the most efficient HTHP configuration are (II) DS S-IHX FT-V2 and (IV) DS D-IHX FT-V2, as sometimes a slight superheating in the IHX 2 is preferable.

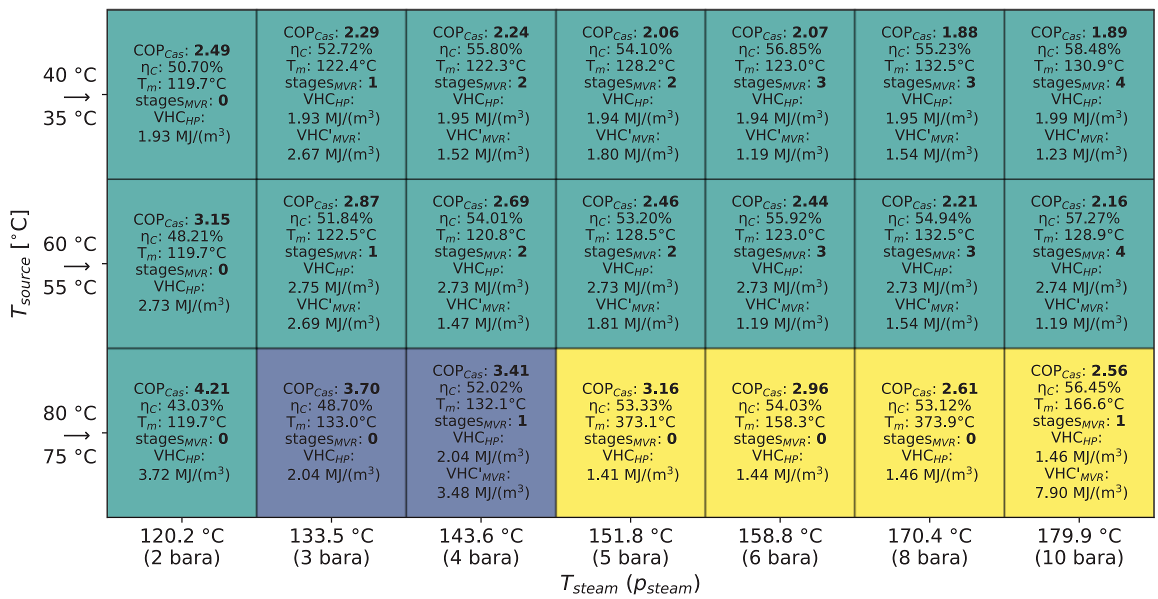


Figure 9: Optimized cascade of alt. HTHP and blower MVR. Applying the same weights for the optimization as in Fig. 8

It is evident that alternative configurations, when combined with a blower VHC, appear well-suited to significantly reduce both the number of MVR stages and the associated structural requirements. However, substantial improvements in efficiency, and thus in the coefficient of performance (COP), are not to be expected. This limitation is rooted in the already high efficiency of the intercooled MVR system, which is partially or entirely substituted by the alternative HTHP.

## 4. Conclusion

This study presents a simulation-based evaluation of two-stage HTHPs with flash tank configuration, tailored to the thermophysical properties of hydrocarbons. Under steady-state conditions and realistic technical constraints, these systems demonstrate clear performance advantages at moderate and variable temperature levels. Notably, temperature lifts exceeding 60 K yield significant improvements regarding COP in a range of 25–50% compared to a theoretical single-stage reference cycle using the same refrigerant. The VHC improvements are comparably lower, but for lifts below 60 K the VHC is likely to decrease. Among the configurations analyzed, variant (I) DS S-IHX FT-V1 is found non-competitive due to its limited performance at equal complexity. While variant (IV) DS D-IHX FT-V2 offers only marginal benefits over variant (II) DS S-IHX FT-V2 under steady-state conditions, the inclusion of a second IHX at intermediate temperature level may provide operational robustness during transient loads or start-up phases. This is particularly relevant when turbo compressors are employed.

When integrated into cascaded systems with downstream blower MVR, these HTHP configurations enable a substantial reduction in the number of MVR stages without compromising COP. This is especially advantageous for source return temperatures below 50 °C, as the higher temperature lift of the HTHP allows for the omission of large MVR stages with high volumetric flow requirements. Refrigerants R600a and R600 are frequently identified as optimal, aligning with their widespread industrial use, which might support rapid deployment of such HTHP-systems. For higher source temperatures or compact system designs without MVR, pentanes (R601a and cyclopentane) appear promising. However, refrigerant selection remains highly sensitive to the chosen evaluation criteria, and the presented results should be interpreted as one possible solution scenario.

The use of COP, VHC, and the number of MVR stages as performance indicators is justified by their strong correlation with both investment and operating costs, and consequently with the LCOH. Currently, the relative weighting of VHC and COP must be defined by the user based on subjective experience. However, electricity consumption typically accounts for 50-80% of the LCOH, highly depending on the electricity prices in each country. An increase in COP of 25% can therefore reduce the LCOH by approximately 10-16%, while a 50% improvement may yield reductions in the range of 17-27%. Adopting the LCOH as the primary evaluation criteria in future studies would eliminate the need for subjective weighting, thereby improving the objectivity and reproducibility of the optimization process. In this context, the suitability of the Nelder–Mead algorithm should be reassessed, as genetic algorithms may offer advantages when addressing the increasing nonlinearity and complexity of the optimization problem. Furthermore, screw or reciprocating compressors represent promising alternatives to blower-based MVR systems for vapor compression.

### Nomenclature

| | | | |
|---|---|---|---|
| so | source | Cmpr | Compressor |
| sk | sink | sat | saturated |
| ref | refrigerant | C | Carnot |
| wt | water | AIT | auto ignition temperature |
| is | isentropic | P | Pinch-Point |
| re | real | NBP | normal boiling point |
| u, $\vec{u}$ | decision variables | w, $\vec{w}$ | weights |
| m | mean | p, $\vec{p}$ | (constant) parameters |


### Acknowledgements

This research was conducted within the project WinPro: “Integration of Closed Heat Pumps into Chemical Industry Processes – Reduction of Primary Energy Demand through Systematic Electrification of Waste Heat Streams” (Förderkennzeichen: 03EN2115B) founded by:

**References**


[1] "Agora Energiewende, Fraunhofer IEG (2023): Roll-out von Großwärmepumpen in Deutschland. Strategien für den Markthochlauf in Wärmenetzen und Industrie.," 2023.

[2] T. Fleiter, M. Rehfeldt, S. Hirzel, L. Neusel and A. Aydemir, "Endbericht: CO2-neutrale Prozesswärmeversorgung," Fraunhofer-Institut für System und Innovationsforschung, Karlsruhe, 2023.

[3] T. Fleiter et al., "Energieverbrauch und CO2-Emissionen," Fraunhofer Verlag, Fraunhofer-Institut für System- und Innovationsforschung ISI, 2013.

[4] C. Mateo-Royo, C. Arpagaus and A. Mota-Babiloni et al., "Advanced high temperature heat pump configurations using low GWP refrigerants for industrial waste heat recovery: A comprehensive study," vol. Energy Conversion and Management, 2021.

[5] M. Sadeghi, T. Peterson, Z. Yang and B. Zühlsdorf et. al., "Thermal and ecnomic performance assement of different high temperature heat pump layouts for upgrading district heating to process heating of steam production at 160°C," vol. Energy, no. 313, 2024.

[6] A. Marina, A. Smeding and S. Wemmers et al., "Design and Experimental Results of a Two-Stage Steam Producing Industrial Heat Pump," vol. 13th IEA Heat Pump Confernce, no. 156, 2021.

[7] B. Donskikh and V. Istomin, "Refined Correlation for Predicting the critical temperature of high boiling normal and branched alkanes," *Teplofizika Vysokikh Temperatur,* vol. 62, no. 62, pp. 846-888, 2024.

[8] M. Caramaschi, J. K. Jensen and S. Poppi et al., "Natural refrigerant mixtures in low-charge heat pumps: An analysis of the potential for performance enhancements," *International Journal of Refrigeration,* p. https://doi.org/10.1016/j.ijrefrig.2024.04.016, 2024.

[9] I. Bell, J. Wronski, S. Quoilin and V. Lemort, "Pure and Pseudo-pure Fluid Thermophysical Property Evaluation and the Open-Source Thermophysical Property Library CoolProp," *Industrial & Engineering Chemistry Research,* vol. 6, no. 53, 2014.

[10] C. Arpagaus, Hochtemperatur-Wärmepumpen: Marktüberblick, Stand der Technik und Anwendungspotentiale, Berlin : VDE Verlag GmbH, 2019.

[11] S. Klute, M. Budt, M. van Beek and C. Doetsch, "Steam generating heat pumps - Overview, classifications, economics and basic modeling principles," vol. Energy Conversion and Management, no. 299, 2024.

[12] B. Zühlsdorf, J. K. Jensen, S. Cignitti, C. Madsen and B. Elmegaard, "Analysis of temperature glide matching of heat pumps with zeotropic working fluid mixtures for different temperature glides," vol. Energy, no. 153, 2018.

[13] M. Utri, Dissertataion: Potenzial von nicht-konstanter Rotorsteigung, Dortmund , 2021.

[14] C. Schlemminger and M. Bantle, "Aneo Industry: Integration of a steam generating heatpump with 1,6 MWth output," *DKV Tagung ,* 2024.

[15] Verein Deutscher Ingenieure , *VDI 2076: Economic efficiency of building installations - Fundamentals and economic calculation,* 2012.

[16] G. Towler and R. Sinnott, Chemical Engineering Design: Principles, practice and econmoics of plant and process design, Elsevir, Butterworth-Heinemann, 2022.

[17] A. Vannoni, A. Sorce, A. Traverso and A. F. Massardo, "Large size heat pumps advanced cost functions introducing the impact of design COP on capital costs," vol. Energy, no. 284, 2023.

[18] J. Nocedal and S. J. Wright, Numerical Optimisation, Springer Nature, 2006.

[19] L. Karunanithi and T. Govindarajan, "Global Design Optimization of a refrigerationsystem using a genetic algorithm," vol. SA Journal of Industrial Engineering, 2003.

[20] S. Takenaga, Y. Ozaki and M. Onishi, "Practical initialization of the Nelder–Mead method for computationally expensive optimization problems," vol. Optimization letters, no. 297, 2023.